

A Capacitance Measurement System Using an IVD Bridge[†]

Speaker: Bryan C. Waltrip
100 Bureau Drive, MS 8111
bryan.waltrip@nist.gov

Authors:

Bryan C. Waltrip and Andrew D. Koffman
National Institute of Standards and Technology[‡], Gaithersburg, MD 20899-8111

Svetlana Avramov-Zamurovic
U.S. Naval Academy, Annapolis, MD 21402

Abstract: A new system to characterize the magnitude and phase characteristics of 1 pF to 1 μ F capacitance standards over the 50 Hz to 100 kHz frequency range is described. The system has been developed to provide measurement support for LCR meters and general impedance measurement services. It consists of an inductive voltage divider (IVD) bridge capable of accurately comparing two capacitance standards and a set of 1 pF to 1 nF capacitance standards with known magnitude and phase characteristics. Details of the measurement system will be given, along with preliminary measurement results and major sources of error.

Introduction

The Electricity Division at the National Institute of Standards and Technology (NIST) is developing expanded impedance measurement services for its customers. There is a growing demand for measurements supporting commercial impedance meters over a broader frequency range than previously offered by NIST. The effort to meet this demand has lead Electricity Division staff to apply the NIST Binary Inductive Voltage Divider (BIVD) Bridge ⁽¹⁻³⁾ to the measurement of capacitance standards. The bridge is intended to measure both four-terminal-pair and high-accuracy three-terminal standards. More correctly, the bridge compares an unknown standard against a known standard using an IVD set to an appropriate ratio, enabling an accurate scaling of capacitance measurement. The bridge has been successfully operated at frequencies from 50 Hz to 100 kHz for IVD ratio measurements ⁽³⁾, although preliminary capacitance measurements have been performed only at 1 kHz and 10 kHz. Key attributes of the BIVD Bridge include fully automatic operation, in-phase and quadrature (magnitude and phase) characterization (thus loss can be determined using an appropriate loss standard), and sensitivity (resolution) for both the in-phase and quadrature components of well below a part in 10^6 . For in-depth ac bridge theory, see *Coaxial AC Bridges*, by Kibble and Rayner ⁽⁴⁾.

[†] Contribution of the U.S. Government. Not subject to copyright in the U.S.

[‡] Electronics and Electrical Engineering Laboratory; Technology Administration; U.S. Department of Commerce.

IVD Bridge System

The bridge system consists of a dual-channel voltage source, SOURCE A and SOURCE B (one channel to drive the bridge and the second to provide the quadrature injection signals); a reference IVD, RIVD, and associated drive IVD, DIVD; a standard and a test capacitor, C_S and C_T ; several injection-control IVDs, IVD1-IVD4, and associated injection transformers, IT1-IT4; tuned null detectors, DET1-DET2; resistive voltage dividers, R_1/R_2 and R_3/R_4 , and a detection transformer, DT, as shown in Fig. 1.

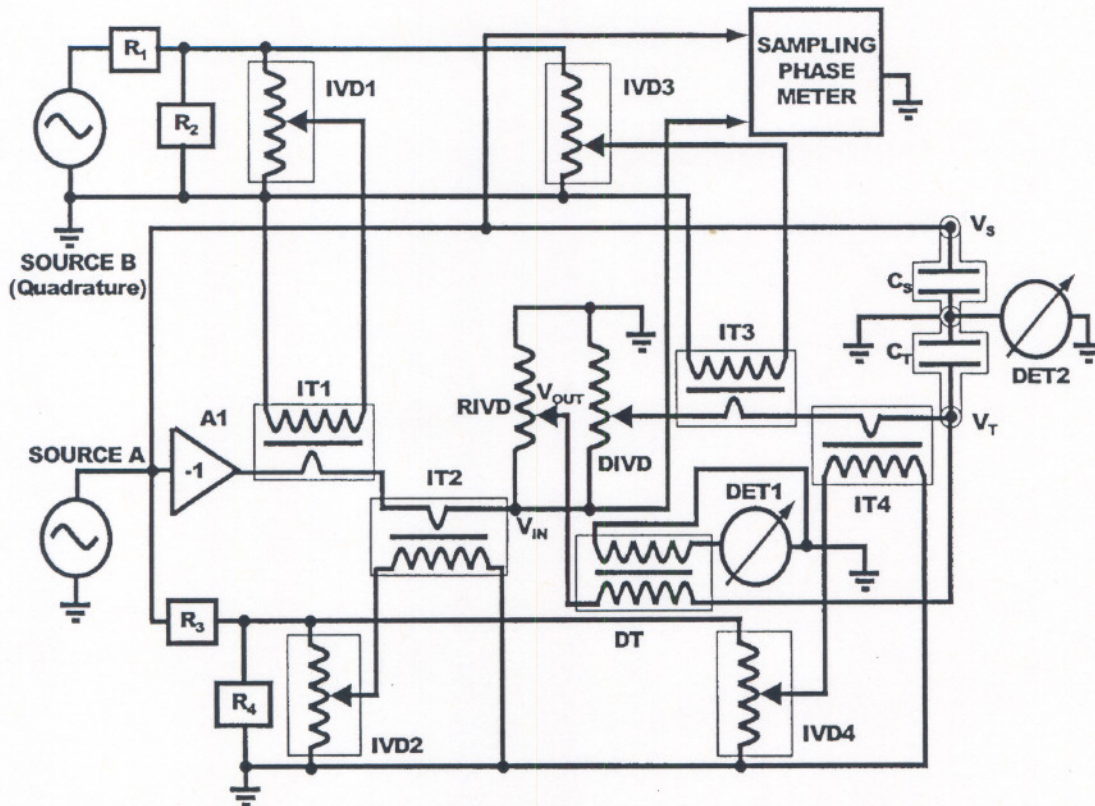


Figure 1. Capacitance scaling bridge.

The bridge is configured with all arms ground-referenced. The first two arms of the bridge consist of the in-phase SOURCE A signal driving the standard capacitor, C_S , and the other two arms are made up of an inverted-phase signal (at the output of inverting amplifier A1) driving the reference IVD, RIVD, the drive IVD, DIVD, and the test capacitor, C_T . The output tap of the RIVD is isolated from C_T using unloading circuitry, consisting of DIVD, IT3, IT4, and DT. A binary inductive voltage divider (BIVD) with very high resolution (30 bits) and accuracy is used as the reference IVD⁽³⁾.

The bridge requires two separate balances to determine the value of C_T , relative to C_S . The first balance involves adjusting the RIVD and DIVD settings until the center point of C_S and C_T is

near a virtual ground, within the resolution of the IVDs, as determined by detector DET2 (a tuned null detector). IVD2 and IVD1 are then adjusted to provide the residual in-phase and quadrature injection signals (injected through IT2 and IT1) necessary to achieve a more exact virtual ground condition. The second balance is necessary to ensure that no current is drawn from the output tap of the RIVD. The output of the DIVD is set to the same nominal ratio as the RIVD, and IVD4 and IVD3 are then adjusted to provide the residual in-phase and quadrature injection signals (injected through IT4 and IT3) necessary to drive the voltage at the high terminal of C_T to equal the voltage at the RIVD tap, i.e., to force the condition $V_{OUT} = V_T$. Detector DET1 (a tuned null detector) senses the imbalance between V_{OUT} and V_T through the isolation and detection transformer, DT.

Voltage dividers R_1/R_2 and R_3/R_4 divide the SOURCE A and SOURCE B signals down to a suitably small level to improve the effective resolution of the in-phase and quadrature injection IVDs. Detectors DET1 and DET2 are synchronized to the dual-channel voltage source, SOURCE A and SOURCE B, using a TTL reference signal from the source (not shown in Fig. 1).

All components of the bridge are operated under remote control using an IEEE-488 interface bus. The two bridge balances are performed automatically under software control.

After the bridge has been balanced, a sampling phase meter ⁽⁵⁾ (shown in Fig. 1) is used to determine the amplitude ratio and phase relationship between the V_S and V_{IN} signals. When measuring sinewave signals of nearly equal amplitude, it has been shown that this phase meter can accurately estimate the amplitude ratio of the two signals to better than 2 parts in 10^6 and the phase between them to less than 10 μ radians over the 10 Hz to 100 kHz frequency range. Since the RIVD setting gives a relationship between V_{OUT} and V_{IN} , the relationship between C_S and C_T is given by:

$$C_T / C_S = K_{PM} / K_{RIVD}, \quad (1)$$

where K_{PM} is the ratio of the amplitude of V_S to V_{IN} measured by the sampling phase meter and K_{RIVD} is the setting of the RIVD at a balance.

The loss tangent, $\tan(\delta_T)$, of C_T is given by:

$$\tan(\delta_T) = \tan(\theta_{PM}) + \tan(\delta_S), \quad (2)$$

where θ_{PM} is the phase between V_S and V_{IN} , measured by the sampling phase meter and $\tan(\delta_S)$ is the loss tangent of C_S .

Sources of Error

A detailed error analysis for the IVD Bridge has not yet been performed. However, the results of several capacitance comparisons using several different IVD types as the reference IVD indicate that the errors of this bridge are dominated by the IVD errors. Previous results of an error decomposition between the binary IVDs used in this bridge and commercial decade IVDs show that the binary IVDs exhibit integral non-linearity errors of 0.3 parts in 10^6 for the in-phase

component and 2 parts in 10^6 for the quadrature component, at 1592 Hz. These errors increase to 5 parts in 10^6 for the in-phase component and 12 parts in 10^6 for the quadrature component, at 10 kHz ⁽¹⁾. Although not shown in equations (1-2), the IVD error contribution to the C_T and $\tan(\delta_T)$ estimation errors depends on the C_S/C_T capacitance ratio. For example, for a $C_S/C_T = 1/10$ capacitance ratio, a 1×10^6 error in the RIVD ratio will translate to a 1×10^5 error in the estimated C_T value.

Preliminary Results

Table 1 presents preliminary capacitance measurement data comparing capacitance ratio and loss tangent difference from the IVD Bridge with that of a commercial capacitance bridge, at frequencies of 1 kHz and 10 kHz. The capacitance values used in the tests were 100 pF and 1 nF. Since the IVD Bridge is a ratio bridge, a characterized standard is needed to provide a measurement result for a test capacitor. Therefore, in this paper, results are presented as capacitance ratios and loss tangent differences between the standard and test capacitors, at capacitance ratios of 1-to-1 and 10-to-1. The comparison agreement information consists of differences between these quantities for each bridge. The estimated uncertainty of the IVD Bridge measurements were derived directly from the error estimates for the in-phase and quadrature components of the reference IVD.

Table 1. Preliminary measurement results.

Freq in kHz	Nom Cap Ratio	Measurements with IVD Bridge (\pm estimated uncertainty)		Measurements with Commercial Bridge		Agreement in Cap Ratios in parts in 10^6	Agreement in Loss Difference
		Capacitance Ratio	Loss Difference	Cap Ratio	Loss Diff		
1	1	0.9999998 ± 0.0000006	$3.2 \times 10^{-6} \pm 4 \times 10^{-6}$	0.9999994	1.6×10^{-6}	0.4	1.6×10^{-6}
1	10	10.000041 ± 0.00006	$6.4 \times 10^{-6} \pm 4 \times 10^{-5}$	10.000063	0.5×10^{-6}	-2.2	5.9×10^{-6}
10	1	0.9999986 ± 0.00001	$3.4 \times 10^{-6} \pm 1.2 \times 10^{-5}$	0.9999984	2.3×10^{-6}	0.2	1.1×10^{-6}
10	10	10.000121 ± 0.001	$14.3 \times 10^{-6} \pm 1.2 \times 10^{-4}$	10.000062	0.6×10^{-6}	5.9	13.7×10^{-6}

Ongoing Work

The bridge setup for capacitance measurements must be characterized completely for measurements from 50 Hz to 100 kHz. As shown in Fig. 1, the IVD Bridge compares the voltage ratios of a reference IVD to a capacitive divider, consisting of the standard and test capacitances. Presently, the reference IVD is a high-resolution (30-bit) binary divider. Future plans include designing and constructing new binary and decade reference IVDs with lower in-phase and quadrature errors. The new IVDs will likely have lower resolution than the present designs in order to achieve the improved accuracy goals. Since the sampling phase meter used in this bridge is able to accurately resolve amplitude ratio differences of nearly equal-amplitude signals, the decreased resolution of the reference IVD is acceptable. An error decomposition will then be performed to distinguish the errors of the new binary IVD from those of the new decade IVD, similar to the methods described in reference (6), to accurately estimate and compensate bridge errors due to the reference IVD.

References

- (1) Avramov, S., "Voltage Ratio Measurements Using Inductive Voltage Dividers," Doctoral Dissertation, University of Maryland Electrical Engineering Department, 1994, College Park, MD.
- (2) Avramov, S., Oldham, N. M., and Gammon, R. W., "Inductive Voltage Divider Calibration for the NASA Flight Experiment," Proceedings of the National Conference of Standards Laboratories (NCSL), July 25-29, 1993, Albuquerque, NM, pp. 225-232.
- (3) Avramov, S., Oldham, N. M., Jarrett, D. G., and Waltrip, B. C., "Automatic Inductive Voltage Divider Bridge for Operation from 10 Hz to 100 kHz," IEEE Trans. Inst. and Meas., Vol. 42 No. 2, April 1993, pp. 131-135.
- (4) Kibble, B. P. and Rayner, G. H., *Coaxial AC Bridges*, Adam Hilger Ltd., 1984, Techno House, Redcliffe Way, Bristol BS1 6NX.
- (5) Waltrip, B. C., "The NIST Sampling System for the Calibration of Phase Angle Generators from 1 Hz to 100 kHz," Proceedings of the National Conference of Standards Laboratories (NCSL), July 1992, pp. 613-616.
- (6) Avramov-Zamurovic, S., Stenbakken, G. N., Koffman, A. D., Oldham, N. M., and Gammon, R. W., "Binary vs. Decade Inductive Voltage Divider Comparison and Error Decomposition," IEEE Transactions on Instrumentation and Measurement, Vol. 44, No. 4, August 1995, pp. 904-908.